An engineered imine reductase for highly diastereo- and enantioselective synthesis of β-branched amines with contiguous stereocenters

Zhen-Yu Zhu
East China University of Science and Technology
Min Shi
East China University of Science and Technology
Yun-Fei Gao
East China University of Science and Technology
Xin-Yuan Shen
East China University of Science and Technology
Xu-Wei Ding
East China University of Science and Technology
Chen-Lin Li
East China University of Science and Technology
Fei-FeiChen
East China University of Science and Technology https://orcid.org/0000-0002-8567-2054
Jian-He Xu
East China University of Science and Technology https://orcid.org/0000-0003-0140-3808
Qi Chen
chenq@ecust.edu.cn

East China University of Science and Technology
Gao-Wei Zheng
gaoweizheng@ecust.edu.cn

East China University of Science and Technology https://orcid.org/0000-0001-5918-6047

Research Article

Keywords: biocatalysis, dynamic kinetic resolution, reductive amination, imine reductase, tofacitinib, protein engineering

Posted Date: April 22nd, 2024

DOI: https://doi.org/10.21203/rs.3.rs-4290287/v1

Additional Declarations: The authors declare no competing interests.

Abstract

βBranched chiral amines with contiguous stereocenters are valuable building blocks for preparing various biologically active molecules. However, their asymmetric synthesis remains challenging. Herein, we report a highly diastereo- and enantioselective biocatalytic approach for preparing a broad range of β-branched chiral amines starting from their corresponding racemic ketones. This involves a dynamic kinetic resolution-asymmetric reductive amination process catalyzed using only an imine reductase. Four rounds of protein engineering endowed wild-type *Poc*IRED with higher reactivity, better stereoselectivity, and a broader substrate scope. Using the engineered enzyme, various chiral amine products were synthesized with up to > 99.9% *ee*, > 99:1 *dr*, and > 99% conversion. The practicability of the developed biocatalytic method was confirmed by producing a key intermediate of tofacitinib in 74% yield, > 99.9% *ee*, and 98:2 *dr* at a challenging substrate loading of 110 g L^{-1}. Our study provides a highly capable imine reductase and a protocol for developing an efficient biocatalytic dynamic kinetic resolution-asymmetric reductive amination reaction system.

INTRODUCTION

β-Branched chiral amines containing contiguous stereocenters are widespread in biologically active molecules including pharmaceuticals lirexapride, moxifloxacin, and tofacitinib (Fig. 1a).[1] For example, (3*R*,4*R*)-1-benzyl-*N*,4-dimethylpiperidin-3-amine **2a** (Fig. 1c) serves as a pivotal chiral intermediate in the synthesis of tofacitinib, a protein tyrosine kinase inhibitor for treating rheumatoid arthritis, active psoriatic arthritis, and ulcerative colitis.[2] However, their highly diastereo- and enantioselective synthesis remains challenging due to the simultaneous construction of multiple stereocenters. Traditional chemical methods typically rely on complicated resolution of racemic amines, resulting in a theoretical yield only 25%. Asymmetric synthesis methods including dynamic kinetic resolution-asymmetric reductive amination;[3–11] asymmetric reduction-asymmetric reductive amination;[12–16] asymmetric hydroamination[17–20] and asymmetric hydrogenation,[1,7,21] have also been reported (Fig. 1b). However, such methods typically require the use of rare-transition-metal complexes with chiral ligands that are difficult obtain and remove, or a multi-catalyst cascade that makes the reaction system cumbersome. In addition, these methods often require harsh conditions, generate large amounts of waste, and achieve only a moderate turnover number and poor diastereo- and enantioselectivity. Therefore, developing more efficient, direct, and stereoselective methods that efficiently afford β-branched chiral amines is highly desirable.

Enzymatic synthesis is becoming more widespread in industry due to benefits such as mild reaction conditions, remarkable stereoselectivity, and eco-friendly processes.[22–25], Owing to their excellent stability, activity, and stereoselectivity, transaminases have emerged as a universally adopted enzyme platform for chiral amine synthesis.[26–29] However, they are limited to synthesizing primary amines, suffer from thermodynamic equilibrium constraints, and generate numerous by-products.[30] Consequently, increased attention has been directed towards imine reductases (IREDs) as a class of alternative

biocatalysts for the synthesis of various chiral amines involving primary, secondary, and tertiary amines. IREDs are a class of NAD(P)H dependent oxidoreductases that catalyze the direct reduction of prochiral imines and reductive amination of ketones with amines to generate the corresponding (chiral) amines.[10,31–33] Over the last decade, numerous wild-type (WT) imine reductases have been studied for their ability to synthesize amines.[34–40] Unfortunately, WT IREDs generally suffer from poor activity, stability, or stereoselectivity, confining their usage to the laboratory and hindering their widespread application in industry.[31,41,42] To date, only a select few engineered IREDs have been developed for the industrial synthesis of chiral amines, contributing to the manufacture of pharmaceuticals such as the LSD1 inhibitor GSK287955241, abrocitinib, and larotrectinib.[43–45] Notably, in these instances, the resulting products only exist as a single pair of isomers. Few IREDs have been used for the highly efficient synthesis of challenging amine products with multiple stereocenters.[10,11,16,46]

In this study, we identified and engineered an IRED capable of the highly diastereo- and enantioselective synthesis of a broad range of β-branched amines, including the key tofacitinib precursor, through dynamic kinetic resolution-asymmetric reductive amination (DKR-ARA) of racemic ketones (Fig. 1c). For substrates in the present work such as **2**, the main challenges are weaker electron-withdrawal effects of ketones relative to aldehydes[47] and the electron-donating effects of methyl (alkyl) groups adjacent to carbonyl groups; these effects reduce the acidity of α-hydrogens, and hinder the racemization of the substrates via enolization.[48] Furthermore, the binding of small methyl (alkyl) group and enzyme in

active pocket was accomplished only through weaker forces such as van der Waals forces, making it more difficult to afford to resolve the racemic substrates.

RESULTS AND DISCUSSION

Identification of IREDs. To identify suitable IREDs, a direct DKR-ARA of racemic 1-benzyl-4-methylpiperidin-3-one **2** (15 mM, 3 g L^{-1}) with methylamine **a** (200 mM) to access (3*R*,4*R*)-**2a**, the pivotal chiral intermediate *en route* to tofacitinib, was chosen as a model reaction (Fig. 1c). A library screening of 125 IREDs from various sources developed by our laboratory was performed for the above reaction. This yielded six enzymes that catalyzed the target reaction, although **2a** was afforded with poor conversions (2–34%) even with excess amine donor (13 eq.) (Table 1). Among them, *Sv*IRED, RedAm-13, and PIR358 displayed reactivity toward the undesired enantiomer (3*S*,4*S*)-**2a** with outstanding stereoselectivity (96–99% *ee*, 91:9–99:1 *dr*) (Table 1, **entries 3–6**). Only *Poc*IRED, IRED-7, and IRED-18 afforded the desired enantiomer (3*R*,4*R*)-**2a** (Table 1, **entries 1 and 2**). However, the hits exhibited low conversion, and insufficient diastereo- and enantioselectivity, which limit their further utility in the efficient synthesis of the tofacitinib precursor. Therefore, reaction optimization and enzyme evolution were necessary to improve the process efficiency and the performance of enzymes. Subsequently, we selected *Poc*IRED as the candidate catalyst for subsequent studies due to its superior catalytic performance compared with IRED-7 and IRED-18.

Reaction optimization. Designing an effective DKR-ARA system is a complex task, necessitating the fulfillment of specific requirements: (i) the racemization rate (k_{rac}) should be high enough to match the enzyme-catalyzed reaction rate of the fast-reacting enantiomer (k_{fast});[49] (ii) enzyme-catalyzed reductive amination of prochiral ketones requires outstanding stereoselectivity; (iii) catalysts must exhibit excellent discrimination between two enantiomers for the kinetic resolution of racemic substrates;[50] (iv) enzymes and biologically active compounds in the reaction system must be compatible with the racemization conditions.[51,52]

One pivotal consideration among these requirements is the balance between k_{rac} and k_{fast}. This becomes particularly critical as, in most cases, k_{rac} is lower than k_{fast} in a neutral aqueous solution.[48,51,53] This imbalance may lead to an undesirable process in which the enzyme is compelled to slowly catalyze (*S*)-**2** into path 3 or 4 (Fig. 2a). Consequently, this will result in a lower substrate conversion and poor optical purity of the product even when using an enzyme with superior activity and stereoselectivity.[9] We sought to address this challenge in two ways. Initially, we tried to adjust the enzyme catalytic rate (k_{fast}) by changing the ratio of substrate to enzyme (S/C) to match the racemization rate. As shown in Fig. 2b (**Entries 1**–**4**), the increase in S/C from 2:1 to 200:1 resulted in the increase in enantiomeric excess and diastereomeric ratio of product from 74% *ee* and 90:10 *dr* to 88% *ee* and 92:8 *dr*, respectively, but the conversion significantly dropped from 95–22%. Elevated pH potentially facilitates the formation of imine intermediates and expedites racemization of substrate enantiomers.[42,51] The results indicated that raising the pH from 8.0 to 9.5 increased *ee* from 82–89%, and enhanced the conversion from 84–91%, confirming our hypotheses (Fig. 2b, **Entries 5–7**). The favorable reaction outcomes (88% *ee*, 92:8 *dr*, 91% conversion) at pH 9.5 with S/C 10:1 strongly support the feasibility of DKR-ARA (fulfilling requirement i).

Protein engineering. Despite achieving promising results through reaction optimization, further protein engineering was clearly needed to enhance the application potential of the biocatalytic process. Meeting process targets for industrial-scale production of the tofacitinib intermediate is imperative, including > 100 g L^{-1} substrate loading, > 90% conversion, > 99.5% *ee* and > 95:5 *dr*.[43,51,54] In addition, since high pH accelerates substrate racemization, it is necessary to improve the tolerance of *Poc*IRED under the high pH conditions that are beneficial for the DKR process. Due to the demanding process targets, it is imperative to concurrently evolve multiple properties of the catalyst including enantioselectivity, diastereoselectivity, activity and tolerance. Therefore, a comprehensive strategy for protein engineering was devised. This included protein crystal structure-based and computational-based approaches for initial site selection, coupled with diverse mutant library design and screening methods.

Initially, the crystal structure of the *Poc*IRED-WT, in complex with $NADP^+$ and substrate **2**, was determined at a resolution of 1.5 Å (PDB: 8YXQ). In the first round, a focused mutant library at 48 sites (the core layer, Fig. 3a) within 9 Å of the substrate-binding pocket was derived by altering amino acids to alanine (A), leucine (L), or phenylalanine (F), respectively in a probe-like fashion.[55] Changes in stereoselectivity were then analyzed using chiral gas chromatography. Sites showing enhanced stereoselectivity underwent single-site saturation mutagenesis, streamlining the evolutionary process to enhance enzyme

stereoselectivity. Several hits with improved stereoselectivity over WT were identified. The most beneficial mutant, Q239G (designated as M1), exhibited markedly improved stereoselectivity, with *ee* increasing from 88% to > 99.9%, and *dr* from 9:1 to 13:1. Furthermore, M1 displayed a 1.8-fold enhancement in conversion compared with its WT.

In the first round of stereoselectivity screening, multiple mutants exhibited an increased *dr* value coupled with decreased conversion or *vice versa*, implying a potential trade-off between diastereoselectivity and conversion. In the second round, these single-point mutants were incorporated into M1 in pursuit of enhanced mutants. However, the trade-off persisted even after combinatorial mutations such as M1 + S72D, M1 + S72N, and M1 + M179G (Fig. 3c). Moderate diastereoselectivity with the sole remaining undesired stereoisomer, (3*R*,4*S*)-**2a** suggested that the mutant successfully accomplished the asymmetric reductive amination of the prochiral carbonyl of **2** (*ee* > 99.9%), yet its capability to discriminate between the enantiomers of the substrate (*rac*-**2**) remained constrained (only fulfilling requirement ii). Therefore, we sought to enhance the diastereoselectivity of the enzyme in the second round of protein engineering. Subsequently, a combinatorial library, combining beneficial single-site mutations from round 1 and a CAST library,[56] was constructed and screened. A single-site mutant, M1 + P125T (designated as M2), was obtained that exhibited an excellent *dr* value (99:1) and maintained enantioselectivity (> 99.9% *ee*), albeit with a decrease in conversion compared to M1. The remarkable *dr* value indicated that productive catalysis with M2 only takes place with an enantiomer of the racemic substrate (fulfilling requirement iii).

Close proximity between the enzyme's active pocket amino acid residues and the substrate undoubtedly increases the likelihood of potentially modifying the enzyme's catalytic properties. Therefore, in the third round, the 48 sites in the first round were chosen again for mutagenesis using the NNK codon set. A random subset of 4600 variants, with 96 mutants per site to cover 20 amino acids with 95% probability,[57] was screened by HPLC to assess conversion under defined reaction conditions (30 g L^{-1} substrate **2** and 600 mM amine donor **a** in pH 9.0 Tris-HCl buffer). Meanwhile, 110 sites from the middle and outer layers of the enzyme active pocket were chosen for saturation mutagenesis (Fig. 3a). For these sites, however, a library-building approach for triple-code saturation mutagenesis was employed, screening only 48 mutants per site to encompass the full range of amino acids with 85% probability.[57,58] This suggests that saturating mutagenesis at 110 sites only required the screening of 5280 mutants. Utilizing *in silico* protein structure analysis, the efficiency of protein engineering can be significantly enhanced by determining the potential influence of different sites on enzyme catalytic performance and subsequently employing diverse saturation mutagenesis methods. In addition, various computer-assisted methods, including identity analysis and homology comparison with engineered imine reductases, were employed in this round to identify potentially beneficial hits.[45] Numerous positive mutations, resulting in a 1.2- to 4-fold improvement in conversion, were obtained compared with M2.

While beneficial mutants can be rapidly identified through single-point mutations, potential multi-point mutants with synergistic effects may be overlooked. Hence, in the fourth round, beneficial mutations from the third round were categorized into seven groups based on spatial distance, and mutant libraries were

serially constructed and screened (Fig. 3b, **from group 1 to group 7**) within each group using multicodon combinatorial mutagenesis (see **Fig. S7**, and **Table S6** for details).[59] The screening pressure is raised incrementally to converge toward the desired process conditions (substrate loading from 30 to 80 g L^{-1}, methylamine concentration from 600 mM to 1200 mM, pH from 9.0 to 9.5). Screening of these libraries under process-like conditions provides variants that are incrementally better adapted to the desired process conditions.[28,60] After several iterative rounds of combinatorial mutation library screening, the catalytic activity and tolerance of the IRED was substantially improved.

The results and screening pressure are summarized in Fig. 3d. The initial two rounds prioritized enhancing the enzyme's stereoselectivity, with mutant M2 exhibiting flawless stereoselectivity and a two-fold rise in specific activity compared with WT. The subsequent two rounds focused on improving catalyst activity and tolerance (**mc**). Following thorough screening, a 20-point mutant variant, *Poc*IRED-M6 (Q239G; P125T; S40E; V124T; I127E; L128Y; S72N; Y73Q; T76V; K195A, G180S, R220V, A47P, V50A, F210L, K212A, W217Q, I178V, H224R; L236I), was identified. M6 displayed outstanding diastereo- and stereoselectivity (> 99.9% *ee* and > 99:1 *dr*, compared with WT 88% *ee* and 9:1 *dr*), high specific activity (6.4 U mg^{-1}, compared with 0.34 U mg^{-1} for WT), and thermostability (T_m 63.5°C vs. T_m 48.1°C for WT). Moreover, M6 exhibited enhanced robustness for high pH (fulfilling requirement iv), increased tolerance to methylamine and cosolvent DMSO, and improved expression in the *Escherichia coli* host (**Fig. S5**, **Fig. S6**, and **Fig. S16**). The criteria for establishing a DKR-ARA system through reaction optimization and protein engineering were satisfactorily fulfilled, and the next step involved evaluating the performance of the system.

Substrate scope. With the best mutant M6 in hand, we subsequently explored the substrate scope of the tailored *Poc*IRED and WT (Table 2). In general, M6 exhibited a broader substrate scope and enhanced catalytic performance compared with WT. We initially investigated the asymmetric synthesis of **2b**–**2i** via IRED-catalyzed biotransformation of ketone **2** with various amine nucleophiles (**b**–**i**). The results showed that M6 exhibited outstanding enantioselectivity (95–99% *ee*), and diastereoselectivity (98:2 to 99:1 *dr*) toward all amine donors tested, even ammonia. By contrast, WT exhibited very low conversion and poor stereoselectivity toward almost all amine donors. Less than 10% conversion was obtained with amine donors **b**–**d, f** and **g** and no detectable product was formed for **e** and **h.** For ketones **1**–**4**, conversion with both M6 and WT progressively decreased with increasing steric hindrance of the β-substituted group.

Finally, substrates bearing additional functional groups on their aromatic ring **5**–**20** were tested with both WT and M6. We found that various ketones were smoothly acted on by M6 to generate the corresponding products with excellent enantioselectivity (> 99% *ee*) and high diastereoselectivity (93:7–99:1 *dr*). The results indicate that the position of the substituent (*ortho*, *meta*, *para*), an electron-withdrawing or electron-donating group, had no significant effect on the performance of M6. Notably, we successfully improved the diastereoselectivity of **16a** from 79:21 to 93:7 under optimized S/C conditions, suggesting the possibility of further improving stereoselectivity through reaction optimization. By contrast

WT displayed distinct catalytic activities toward different ketones. In general, ketones with substituent at the *meta* position on the benzene ring were better tolerated than those at the *para* and *ortho* positions. Among the seven *para*-substituted substrates (**5, 9, 13**, and **17**–**20**), WT only exhibited favorable catalytic performance toward ketone **9**, but showed poor or reversed stereoselectivity, or even no activity, toward others. These results may be attributed to steric hindrance, with the smaller hindrance of a fluorine atom substituent in the *para* position (substrate **9**) having less impact on WT catalytic performance. In addition, WT displayed a near loss of stereoselectivity for *ortho* position substrates **7, 11** and **15**. In conclusion, the engineered M6 has a broader substrate acceptance scope and better selectivity than WT, making it a promising biocatalyst for the highly diastereo- and enantioselectivity synthesis of β-branched chiral amines with contiguous stereocenters.

Preparative synthesis of the tofacitinib intermediate. To demonstrate the utility of the developed biocatalytic method, a preparative synthesis of the tofacitinib intermediate was conducted at a substrate concentration of 110 g L^{-1} in a 500 mL reaction volume, using the best mutant M6 in the form of lyophilized cell-free extract. The reaction was maintained at pH 9.5 through titration with a 1.5 M aqueous methylamine solution.[61] Subsequently, *Poc*IRED-M6 facilitated the reductive coupling of rac-**2** (110 g L^{-1}, 550 mM) with methylamine (1000 mM, 1.8 eq.), yielding 44.5 g of product with > 99.9% *ee*, 98:2 *dr*, and a yield of 74% **(**Fig. 4**)**. These results demonstrate superior stereoselectivity and substrate loading compared with previously reported enzyme- or chemical-catalyzed asymmetric synthesis of the tofacitinib intermediates.

Mechanistic analysis. To gain insight into the mechanism of the improvement of the engineered catalyst, X-ray crystal structures of *Poc*IRED-M6 with NADPH (PDB: 8YVH), and *Poc*IRED-M6 with NADPH and substrate **2 (**PDB: 8YXY**)** were solved at resolutions of 2.1 and 1.1 Å (**Table S14**), respectively. Furthermore, based on the X-ray structures, molecular dynamics simulations were performed to investigate the structural foundation. The final mutant, *Poc*IRED-M6, contains 20 mutation sites, with 12 sites from the core layer of the mutant library and 8 from the middle or outer layers. Mutations V124T, P125T, I127E, L128Y, G180S, F210L, W217Q, R220V, H224R, L236I, and Q239G are situated within the active pocket, and might be mainly involved in substrate- and cofactor- binding, as well as stereoselective catalysis. Mutations S40E, A47P, V50A, T76V, K195A, and K212A are located on the surface or distal side of the protein, potentially contributing to increased hydrophilicity or charge of the protein surface and decreased flexibility, thereby favoring enzyme expression and stability. Mutation A47P is located at the end of a loop, where proline probably aids in stabilizing the loop and mutation T76V results in an elongation of the α-helix (**Fig. S22**), thereby enhancing structural stability. In addition, mutation I178V probably also intensifies the rigidity by stabilizing the dimer interface. Other mutations, namely S72N and Y73Q are close to the cofactor and might influence its positioning **(**Fig. 5a**)**.

Mutations are distributed across various regions of the enzyme. They not only tailor the active pocket for the catalytic steps (chemical steps), but also modify the overall structure for the physical steps of the catalytic cycle, which involve substrate access and product release. From a crystallographic perspective, the active pocket of the ternary complex *Poc*IRED-M6 (binding NADPH and substrate) exhibited a more

compact conformation compare with the binary complex that only binds NADPH (**Fig. S21)**. However, *Poc*IRED-WT maintained its closed form of the pocket regardless of the presence of binding substrates (**Fig. S19c**). Substrate inhibition generally attributed to the formation of an unproductive enzyme–substrate complex after the simultaneous binding of two or more substrate molecules in the active pocket.[62] The closed conformation of WT may result in the unproductive binding of substrates. Indeed, *Poc*IRED-WT exhibited severe substrate inhibition (0.34 U mg^{-1} at 50 mM substrate concentration vs. 0.13 U mg^{-1} at 200 mM), and simultaneously accommodated two substrates **2** in its active pocket (**Fig. S19b**). Compared with the closed form of WT, M6 exhibited two active pocket forms of opening and closing that were activated by the substrate. In addition, the smaller, amino acid side chains of T125 (A), Q217 (B), V220 (B), I236 (B), and G239 (B) also affected the substrate tunnel in M6. New substrate tunnels were observed in M6 **(**Fig. 5d and 5e; **Fig. S14d and S14e)**. This may also be partially accountable for the enhanced catalytic activity and reduced substrate inhibition (6.4 U mg^{-1} at 50 mM substrate concentration vs. 5.2 U mg^{-1} at 200 mM) by improving the physical steps.

According to the molecular dynamics simulation results, the substrate could be stabilized in the binding pocket in both WT and M6 throughout the entire simulation. The substrate-binding affinity of *Poc*IRED-M6 calculated using MMPBSA method was slightly decreased (-20.9 ± 3.7 kcal/mol, -17.6 ± 3.9 kcal/mol in different parallel simulations) compared with that of *Poc*IRED-WT (-23.8 ± 4.4 kcal/mol, -25.0 ± 3.5 kcal/mol) (**Table S10**). Although the substrate can bind in the pocket in both WT and M6, the binding mode differs in these two systems.

In WT, the side chain of W217 (B) engages in aromatic-proline interactions with P125 (A), and π-π stacking interactions with F210 (B). Since P125 (A) is located close to NADPH, the substrate is obstructed and prevented from binding closer to NADPH (Fig. 5b). The distances between C4 atoms of NADPH and substrate C atoms are relatively long and unstable (7.0 ± 1.3 Å and 10.7 ± 0.5 Å in different parallel simulations; **Fig. S12**). By contrast, in M6, the smaller side chains of T125 (A), L210 (B), and Q217(B) alleviate the steric hindrance, allowing the substrate to bind closer to NADPH (Fig. 5c), resulting in a shorter and more stable distances between C4 atoms of NADPH and the prochiral C atoms of the substrate (5.5 ± 0.7 Å and 5.6 ± 0.5 Å in different parallel simulations; **Fig. S13**). Therefore, the substrate in M6 can adopt a more catalytically competent conformation attributed to the tailored active pocket, facilitating the chemical steps.

Finally, we found that compare with WT, M6 formed a salt bridge interaction between R224 (B) and E127 (A), and a stable hydrogen bond between Q217 (B) and T125 (A) **(**Fig. 5b and 5c**)**. These new interactions stabilize the conformation between the two monomers of the enzyme, and are likely to contribute to the improved thermal stability.

Conclusion

An enzymatic asymmetric reductive amination combined with dynamic kinetic resolution method was developed to synthesize β-branched chiral amines containing two consecutive stereocenters

in a single biotransformation. Different saturation mutagenesis strategies were designed and employed based on the potential importance of different residues to rapidly identify hotspots, followed by a zonal iterative combinatorial strategy to integrate single-point mutations to rapidly obtain the most beneficial mutations. This combined structural and computational protein engineering strategy not only reduces the randomness of traditional directed evolution and greatly improves the efficiency of evolution, but could also exploit the evolutionary potential of proteins more effectively than rational design. The final variant M6 displayed substrate loading up to 110 g L^{-1}, conversion up to 93%, and 74% yield, with >99.9% *ee* and 98:2 *dr*. These results demonstrate the effectiveness of the developed protein engineering strategy, especially given the extremely poor starting point (15% conversion at 3 g L^{-1}, with 84% *ee* and 92:8 *dr*). In addition, the engineered M6 has a broader substrate scope and better catalytic ability than WT, and can be used to synthesize a diverse range of β-branched chiral amine moieties. Taken together, these findings are poised to expedite the application of direct reductive amination using engineered IREDs and the development of DKR-ARA systems in the synthesis of chiral building blocks for pharmaceuticals.

Declarations

ASSOCIATED CONTENT

Supporting Information

The Supporting Information is available free of charge at:

Experimental procedures and analyses; bioinformatics data; GC, HPLC, and UPLC chromatograms; mass spectra and NMR spectra (PDF)

AUTHOR INFORMATION

Corresponding Authors

E-mail for Gao-Wei Zheng: gaoweizheng@ecust.edu.cn

E-mail for Qi Chen: chenq@ecust.edu.cn

Author Contributions

G.-W. Z., J.-H. X. and Q. C. devised and supervised the project. Z.-Y. Z. managed the project. Z.-Y. Z. performed enzyme screening, optimization studies, protein engineering and preparative synthesis. Z.-Y. Z., M. S., Y.-F. G., X.-Y. S. and C.-Lw. L. performed substrate scope reactions. M. S. and Z.-Y. Z. performed crystallographic studies. Q. C. carried out molecular dynamics simulation. F.-F. C., Y.-T. X., and X.-W. D. helped guide the project. Z.-Y. Z., F.-F. C. and G.-W. Z. wrote the manuscript. All authors discussed the results and commented on the manuscript.

Competing interests

The authors declare no competing interests.

ACKNOWLEDGMENTS

This work was financially supported by the National Natural Science Foundation of China (32371547 and 22008068) and the National Key Research and Development Program of China (2019YFA09005000 and 2021YFA0911400). We thank BL17B1/BL18U1/BL19U1/ beamline of National Facility for Protein Science in Shanghai (NFPS) at Shanghai Synchrotron Radiation Facility and Prof. R.-T. Guo from Hubei University for assistance during X-ray data collection. We also thank Dr. X.-X. Yuan, Prof. B.-B. Zeng, Dr. C. Ning, Dr. H.-G. Li, and Prof. Y.-T. Xie from East China University of Science and Technology for their kind assistance in chemical synthesis.

References

1. Li, C. et al. Stereoelectronic effects in ligand design: enantioselective rhodium-catalyzed hydrogenation of aliphatic cyclic tetrasubstituted enamides and concise synthesis of (*R*)-tofacitinib. *Angew. Chem. Int. Ed.* **58**, 13573-13583 (2019).
2. Carvalho, L. C. R., Lourenço, A., Ferreira, L. M. & Branco, P. S. Tofacitinib synthesis-an asymmetric challenge. *Eur. J. Org. Chem.* **2019**, 615-624 (2019).
3. Cabrera, A. et al. Diastereo- and enantioselective reductive amination of cycloaliphatic ketones by preformed chiral palladium complexes. *Catal. Sci. Technol.* **4**, 2626-2630 (2014).
4. Rong, Z. Q., Zhang, Y., Chua, R. H. B., Pan, H. J. & Zhao, Y. Dynamic kinetic asymmetric amination of alcohols: From a mixture of four isomers to diastereo-and enantiopure α-branched amines. *J. Am. Chem. Soc.* **137**, 4944-4947 (2015).
5. Lou, Y. Z. et al. Dynamic kinetic asymmetric reductive amination: synthesis of chiral primary β-amino lactams. *Angew. Chem. Int. Ed.* **57**, 14193-14197 (2018).
6. Verzijl, G. K. M., Schuster, C., Dax, T., de Vries, A. H. M. & Lefort, L. Asymmetric synthesis of a key intermediate for tofacitinib via a dynamic kinetic resolution-reductive amination protocol. *Org. Process Res. Dev.* **22**, 1817-1822 (2018).
7. Molinaro, C. et al. Synthesis of a CGPR receptor antagonist via an asymmetric synthesis of 3-fluoro-4-aminopiperidine. *J. Org. Chem.* **84**, 8006-8018 (2019).
8. Rong, Z.-Q. et al. Dynamic kinetic asymmetric amination of alcohols assisted by microwave: stereoconvergent access to tetralin- and indane-derived chiral amines. *ACS Catal.* **10**, 9464-9475 (2020).
9. Li, F. Z., Yang, L. C., Zhang, J. Y., Chen, J. S. & Renata, H. Stereoselective synthesis of β-branched aromatic α-amino acids by biocatalytic dynamic kinetic resolution. *Angew. Chem. Int. Ed.* **60**, 17680-17685 (2021).
10. Marshall, J. R. et al. Screening and characterization of a diverse panel of metagenomic imine reductases for biocatalytic reductive amination. *Nat. Chem.* **13**, 140-148 (2021).

11. Zhan, Z. Z. et al. Stereocomplementary synthesis of a key intermediate for tofacitinib via enzymatic dynamic kinetic resolution-reductive amination. *Adv. Synth. Catal.* **364**, 2380-2386 (2022).
12. Monti, D. et al. Cascade coupling of ene-reductases and ω-transaminases for the stereoselective synthesis of diastereomerically enriched amines. *ChemCatChem* **7**, 3106-3109 (2015).
13. Thorpe, T. W. et al. One-pot biocatalytic cascade reduction of cyclic enimines for the preparation of diastereomerically enriched *N*-heterocycles. *J. Am. Chem. Soc.* **141**, 19208-19213 (2019).
14. Jongkind, E. P. J. et al. Synthesis of chiral amines via a bi-enzymatic cascade using an ene-reductase and amine dehydrogenase. *ChemCatChem* **14**, e202101576 (2021).
15. Knaus, T., Corrado, M. L. & Mutti, F. G. One-pot biocatalytic synthesis of primary, secondary, and tertiary amines with two stereocenters from α,β-unsaturated ketones using alkyl-ammonium formate. *ACS Catal.* **12**, 14459-14475 (2022).
16. Thorpe, T. W. et al. Multifunctional biocatalyst for conjugate reduction and reductive amination. *Nature* **604**, 86-91 (2022).
17. Raj, H. et al. Engineering methylaspartate ammonia lyase for the asymmetric synthesis of unnatural amino acids. *Nat. Chem.* **4**, 478-484 (2012).
18. Zhu, S., Niljianskul, N. & Buchwald, S. L. Enantio- and regioselective CuH-catalyzed hydroamination of alkenes. *J. Am. Chem. Soc.* **135**, 15746-15749 (2013).
19. Shi, S. L., Wong, Z. L. & Buchwald, S. L. Copper-catalysed enantioselective stereodivergent synthesis of amino alcohols. *Nature* **532**, 353-356 (2016).
20. Kang, H. J., Lee, C. & Hong, S. Nickel-catalyzed kinetic resolution of racemic unactivated alkenes via enantio-, diastereo-, and regioselective hydroamination. *Angew. Chem. Int. Ed.* **62**, e202305042 (2023).
21. Kraft, S., Ryan, K. & Kargbo, R. B. Recent advances in asymmetric hydrogenation of tetrasubstituted olefins. *J. Am. Chem. Soc.* **139**, 11630-11641 (2017).
22. Mutti, F. G., Knaus, T., Scrutton, N. S., Breuer, M. & Turner, N. J. Conversion of alcohols to enantiopure amines through dual-enzyme hydrogen-borrowing cascades. *Science* **349**, 1525-1529 (2015).
23. Chen, F. F., Liu, Y. Y., Zheng, G. W. & Xu, J. H. Asymmetric amination of secondary alcohols by using a redox-neutral two-enzyme cascade. *ChemCatChem* **7**, 3838-3841 (2015).
24. Chen, F. F. et al. Reshaping the active pocket of amine dehydrogenases for asymmetric synthesis of bulky aliphatic amines. *ACS Catal.* **8**, 2622-2628 (2018).
25. Chen, F. F. et al. Enantioselective synthesis of chiral vicinal amino alcohols using amine dehydrogenases. *ACS Catal.* **9**, 11813-11818 (2019).
26. Höhne, M., Schätzle, S., Jochens, H., Robins, K. & Bornscheuer, U. T. Rational assignment of key motifs for function guides in silico enzyme identification. *Nat. Chem. Biol.* **6**, 807-813 (2010).
27. Pavlidis, I. V. et al. Identification of (*S*)-selective transaminases for the asymmetric synthesis of bulky chiral amines. *Nat. Chem.* **8**, 1076-1082 (2016).

28. Savile, C. K. et al. Biocatalytic asymmetric synthesis of chiral amines from ketones applied to sitagliptin manufacture. *Science* **329**, 305-309 (2010).
29. Li, J. M. et al. Development of a thermodynamically favorable multi-enzyme cascade reaction for efficient sustainable production of ω-amino fatty acids and α,ω-diamines. *ChemSusChem* **17**, e202301477 (2024).
30. Novick, S. J. et al. Engineering an amine transaminase for the efficient production of a chiral sacubitril precursor. *ACS Catal.* **11**, 3762-3770 (2021).
31. Mitsukura, K., Suzuki, M., Tada, K., Yoshida, T. & Nagasawa, T. Asymmetric synthesis of chiral cyclic amine from cyclic imine by bacterial whole-cell catalyst of enantioselective imine reductase. *Org. Biomol. Chem.* **8**, 4533-4535 (2010).
32. Aleku, G. A. et al. A reductive aminase from *Aaspergillus oryzae*. *Nat. Chem.* **9**, 961-969 (2017).
33. Montgomery, S. L. et al. Characterization of imine reductases in reductive amination for the exploration of structure-activity relationships. *Sci. Adv.* **6**, eaay9320 (2020).
34. Leipold, F., Hussain, S., Ghislieri, D. & Turner, N. J. Asymmetric reduction of cyclic imines catalyzed by a whole-cell biocatalyst containing an (*S*)-imine reductase. *ChemCatChem* **5**, 3505-3508 (2013).
35. Chen, F. F. et al. Discovery of an imine reductase for reductive amination of carbonyl compounds with sterically challenging amines. *J. Am. Chem. Soc.* **145**, 4015-4025 (2023).
36. France, S. P. et al. Biocatalytic routes to enantiomerically enriched dibenz [*c*,*e*] azepines. *Angew. Chem. Int. Ed.* **56**, 15589-15593 (2017).
37. Zhang, Y. H. et al. Stereocomplementary synthesis of pharmaceutically relevant chiral 2-aryl-substituted pyrrolidines using imine reductases. *Org. Lett.* **22**, 3367-3372 (2020).
38. Zhang, J. et al. Tuning an imine reductase for the asymmetric synthesis of azacycloalkylamines by concise structure-guided engineering. *Angew. Chem. Int. Ed.* **61**, e202201908 (2022).
39. Li, Y. et al. Asymmetric synthesis of *N*-substituted 1,2-amino alcohols from simple aldehydes and amines by one-pot sequential enzymatic hydroxymethylation and asymmetric reductive amination. *Angew. Chem. Int. Ed.* **61**, e2021163 (2022).
40. Li, H., Luan, Z. J., Zheng, G. W. & Xu, J. H. Efficient synthesis of chiral indolines using an imine reductase from *Paenibacillus lactis*. *Adv. Synth. Catal.* **357**, 1692-1696 (2015).
41. Huber, T. et al. Direct reductive amination of ketones: structure and activity of *S*-selective imine reductases from *Streptomyces*. *ChemCatChem* **6**, 2248-2252 (2014).
42. Scheller, P. N., Lenz, M., Hammer, S. C., Hauer, B. & Nestl, B. M. Imine reductase-catalyzed intermolecular reductive amination of aldehydes and ketones. *ChemCatChem* **7**, 3239-3242 (2015).
43. Schober, M. et al. Chiral synthesis of LSD1 inhibitor GSK2879552 enabled by directed evolution of an imine reductase. *Nat. Catal.* **2**, 909-915 (2019).
44. Kumar, R. et al. Biocatalytic reductive amination from discovery to commercial manufacturing applied to abrocitinib JAK1 inhibitor. *Nat. Catal.* **4**, 775-782 (2021).

45. Chen, Q. et al. Engineered imine reductase for larotrectinib intermediate manufacture. *ACS Catal.* **12**, 14795-14803 (2022).
46. Steflik, J. et al. Engineering of a reductive aminase to enable the synthesis of a key intermediate to a CDK 2/4/6 inhibitor. *ACS Catal.* **13**, 10065-10075 (2023).
47. Fuchs, C. S. et al. Asymmetric amination of α-chiral aliphatic aldehydes via dynamic kinetic resolution to access stereocomplementary brivaracetam and pregabalin precursors. *Adv. Synth. Catal.* **360**, 768-778 (2018).
48. Cao, J. Z. & Hyster, T. K. Pyridoxal-catalyzed racemization of α-aminoketones enables the stereodivergent synthesis of 1,2-amino alcohols using ketoreductases. *ACS Catal.* **10**, 6171-6175 (2020).
49. Verho, O. & Bäckvall, J. E. Chemoenzymatic dynamic kinetic resolution: a powerful tool for the preparation of enantiomerically pure alcohols and amines. *J. Am. Chem. Soc.* **137**, 3996-4009 (2015).
50. Chen, C. S., Fujimoto, Y., Girdaukas, G. & Sih, C. J. Quantitative analyses of biochemical kinetic resolutions of enantiomers. *J. Am. Chem. Soc.* **104**, 7294-7299 (1982).
51. Xu, F. et al. Synthesis of vibegron enabled by a ketoreductase rationally designed for high pH dynamic kinetic reduction. *Angew. Chem. Int. Ed.* **57**, 6863-6867 (2018).
52. DeHovitz, J. S. et al. Static to inducibly dynamic stereocontrol: the convergent use of racemic β-substituted ketones. *Science* **369**, 1113-1118 (2020).
53. Applegate, G. A. & Berkowitz, D. B. Exploiting enzymatic dynamic reductive kinetic resolution (DYRKR) in stereocontrolled synthesis. *Adv. Synth. Catal.* **357**, 1619-1632 (2015).
54. Wu, S. K., Snajdrova, R., Moore, J. C., Baldenius, K. & Bornscheuer, U. T. Biocatalysis: enzymatic synthesis for industrial applications. *Angew. Chem. Int. Ed.* **60**, 88-119 (2021).
55. Xu, J. et al. Stereodivergent protein engineering of a lipase to access all possible stereoisomers of chiral esters with two stereocenters. *J. Am. Chem. Soc.* **141**, 7934-7945 (2020).
56. Reetz, M. T., Bocola, M., Carballeira, J. D., Zha, D. X. & Vogel, A. Expanding the range of substrate acceptance of enzymes: combinatorial active-site saturation test. *Angew. Chem. Int. Ed.* **44**, 4192-4196 (2005).
57. Reetz, M. T., Kahakeaw, D. & Lohmer, R. Addressing the numbers problem in directed evolution. *ChemBioChem* **9**, 1797-1804 (2008).
58. Sun, Z. T. et al. Structure-guided triple-code saturation mutagenesis: efficient tuning of the stereoselectivity of an epoxide hydrolase. *ACS Catal.* **6**, 1590-1597 (2016).
59. Reetz, M. T. & Carballeira, J. D. Iterative saturation mutagenesis (ISM) for rapid directed evolution of functional enzymes. *Nat. Protoc.* **2**, 891-903 (2007).
60. Bloom, J. D. & Arnold, F. H. In the light of directed evolution: pathways of adaptive protein evolution. *Proc. Natl. Acad. Sci. U. S. A.* **106**, 9995-10000 (2009).

61. Qian, W. Z. et al. Evolution of glucose dehydrogenase for cofactor regeneration in bioredox processes with denaturing agents. *ChemBioChem* **21**, 2680-2688 (2020).
62. Kokkonen, P. et al. Substrate inhibition by the blockage of product release and its control by tunnel engineering. *RSC Chem. Biol.* **2**, 645-655 (2021).

Tables

Tables 1 to 2 are available in the Supplementary Files section

Figures

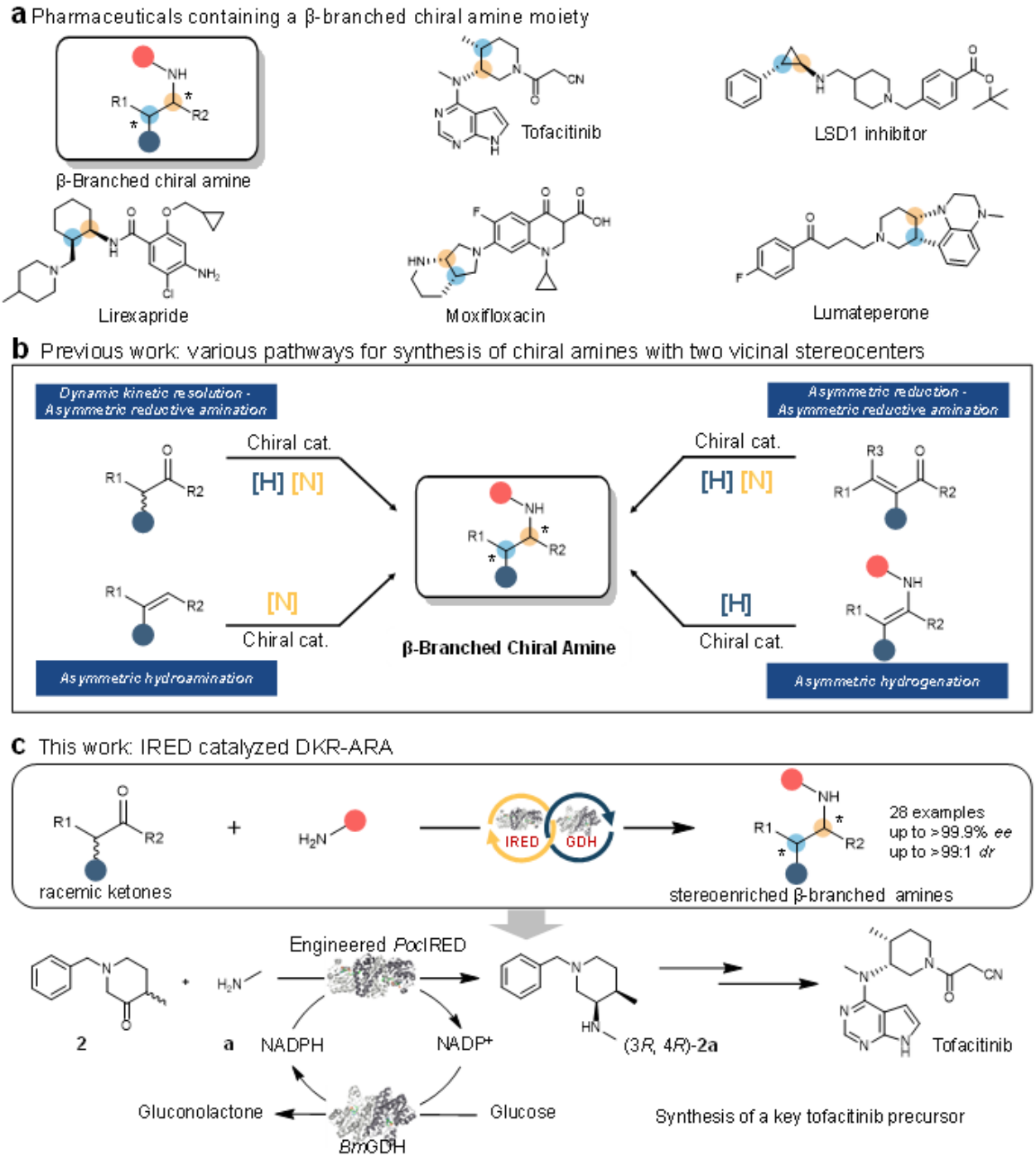

Figure 1

Background and synthetic strategies of β-branched chiral amines. a, Examples of bioactive molecules containing β-branched chiral amines with contiguous stereocenters. **b**, Contemporary methods to prepare β-branched chiral amines. **c**, This work identified and engineered an IRED that enables highly diastereo- and enantioselective synthesis of β-branched amines through dynamic kinetic resolution-asymmetric reductive amination (DKR-ARA), and utilized it for the synthesis of the chiral tofacitinib precursor.

a

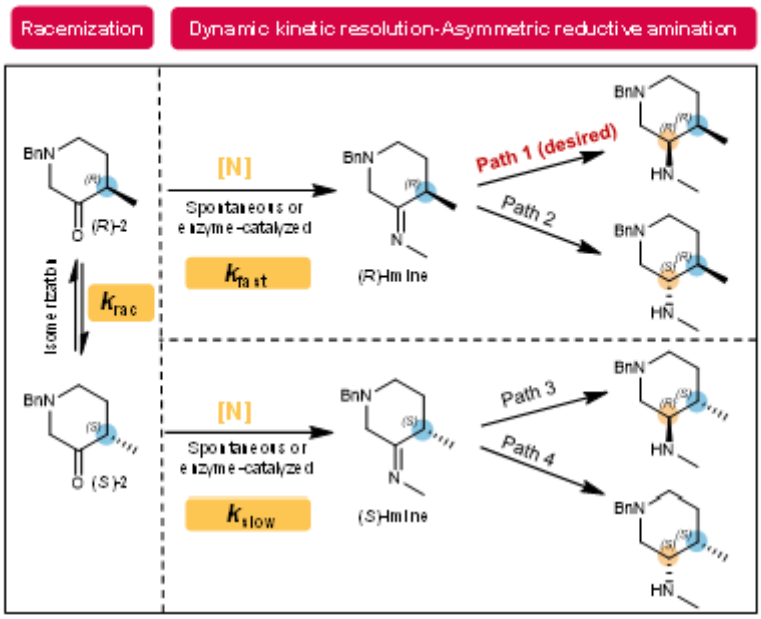

b

Entry	Enzyme	pH	S/C	ee (%)	*dr*	Conv. (%)
1	*Pod*RED	9.0	2:1	74	90:10	95
2	*Pod*RED	9.0	20:1	84	92:8	65
3	*Pod*RED	9.0	100:1	88	92:8	25
4	*Pod*RED	9.0	200:1	88	92:8	22
5	*Pod*RED	8.0	10:1	82	91:9	84
6	*Pod*RED	9.0	10:1	83	92:8	86
7	*Pod*RED	9.5	10:1	89	92:8	91
8	Blank	9.0	-	-	-	0

Figure 2

Optimization studies. a, Proposed mechanism of the DKR-ARA process. **b,** Reaction optimization comprising verification of the proposed mechanism and feasibility of the DKR-ARA process based on the results. S/C: substrate loading/catalyst loading (w/w).

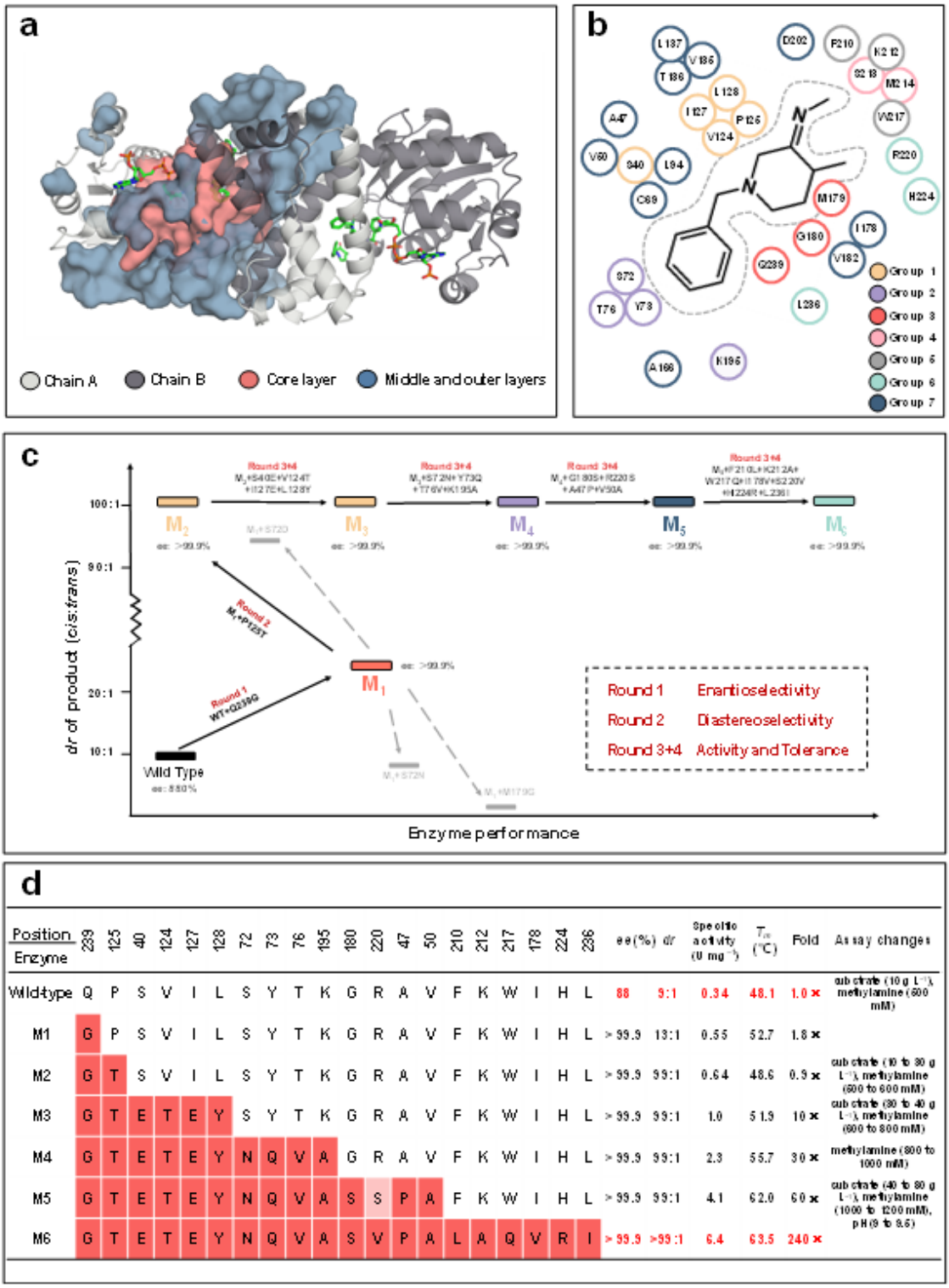

Figure 3

Overview of protein engineering of *Poc*IRED. a, Hierarchy of amino acid residues in the *Poc*IRED structure. **b**, Distribution and grouping of beneficial mutants. **c**, Evolutionary path of *Poc*IRED showing the top hits from each round of protein engineering. **d**, Characterization of WT *Poc*IRED to the final variant M6 from protein engineering. Shades of red indicate that mutations were accumulated in the backbones at the given position in each round of evolution.

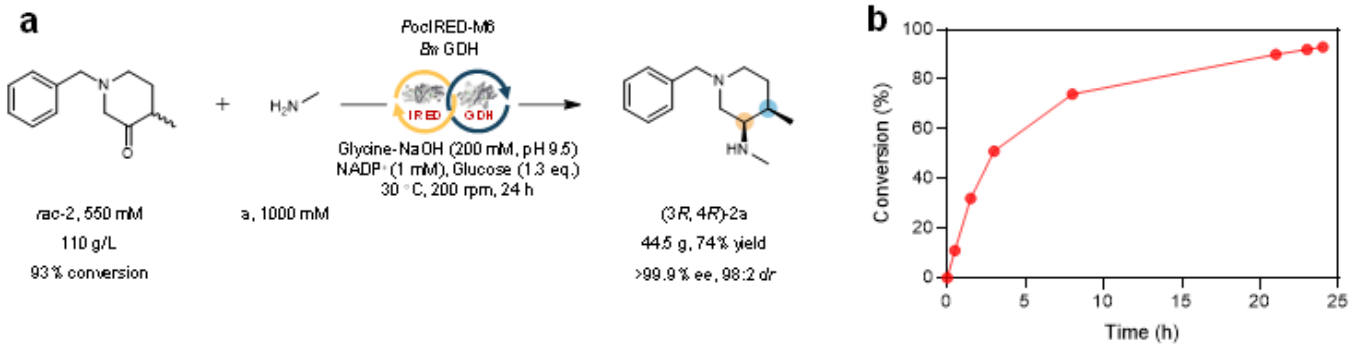

Figure 4

Preparative synthesis. a, preparation of the chiral amine intermediate of tofacitinib using engineered enzyme *Poc*IRED-M6. **b**, reaction profile for conversion versus time.

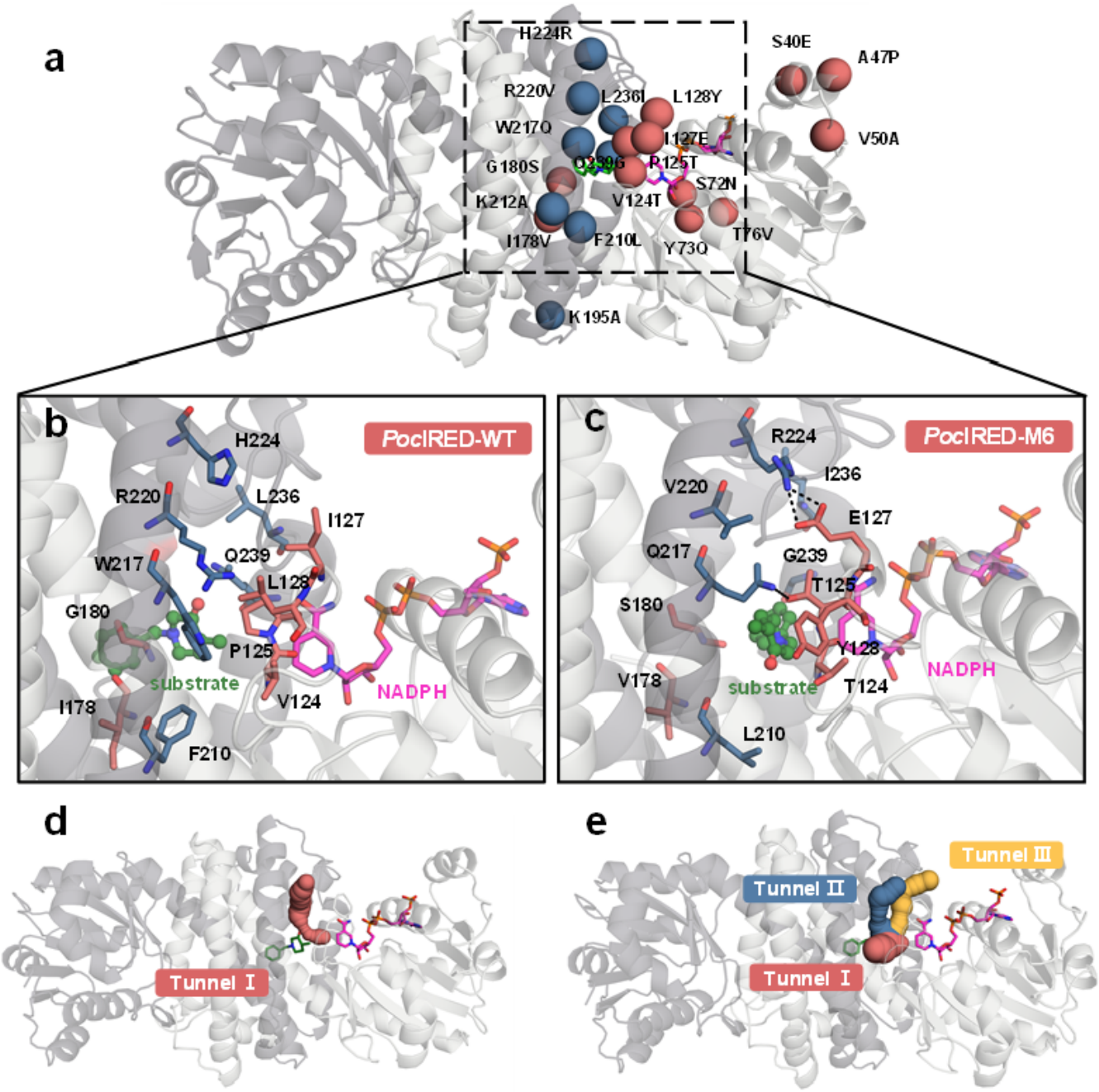

Figure 5

Analysis of structures and mechanisms for *Poc*IRED-WT and its mutant *Poc*IRED-M6. Distribution of all mutated sites (**a**), substrate binding modes of **2** in *Poc*IRED-WT (**b**) and *Poc*IRED-M6 (**c**), and substrate tunnel analysis in *Poc*IRED-WT (**d**) and *Poc*IRED-M6 (**e**).

Supplementary Files

This is a list of supplementary files associated with this preprint. Click to download.

- SupplementaryInformation.docx

- Tables.docx